Check for updates

NANO · MICRO small
www.small-journal.com

Nucleic Acid Enzyme-Activated CRISPR-Cas12a With Circular CRISPR RNA for Biosensing

*Yunping Wu, Dingran Chang, Yangyang Chang, Qiang Zhang, Yi Liu, John D. Brennan, Yingfu Li, and Meng Liu**

clustered regularly interspaced short palindromic repeats (CRISPR)-Cas systems are increasingly used in biosensor development. However, directly translating recognition events for non-nucleic acid targets by CRISPR into effective measurable signals represents an important ongoing challenge. Herein, it is hypothesized and confirmed that CRISPR RNAs (crRNAs) in a circular topology efficiently render Cas12a incapable of both site-specific double-stranded DNA cutting and nonspecific single-stranded DNA trans cleavage. Importantly, it is shown that nucleic acid enzymes (NAzymes) with RNA-cleaving activity can linearize the circular crRNAs, activating CRISPR-Cas12a functions. Using ligand-responsive ribozymes and DNAzymes as molecular recognition elements, it is demonstrated that target-triggered linearization of circular crRNAs offers great versatility for biosensing. This strategy is termed as "NAzyme-Activated CRISPR-Cas12a with Circular CRISPR RNA (NA3C)." Use of NA3C for clinical evaluation of urinary tract infections using an *Escherichia coli*-responsive RNA-cleaving DNAzyme to test 40 patient urine samples, providing a diagnostic sensitivity of 100% and specificity of 90%, is further demonstrated.

1. Introduction

Molecular biosensing is critical for clinical diagnosis, biosecurity, food safety, and environmental monitoring.[1] Recently, clustered regularly interspaced short palindromic repeats (CRISPR) and CRISPR-associated protein (Cas) systems have been increasingly used in biosensor development due to their unique features including high specificity, programmability, compositional versatility, and potential for isothermal amplification.[2] Many CRISPR-based methods have been developed for sensing nucleic-acid-based biomarkers of both infectious and non-infectious diseases.[3] In addition, several CRISPR systems have also been adapted for the detection of a limited number of non-nucleic acid targets such as small molecules, proteins, and metal ions.[4] In these cases, the sensing mechanism is primarily mediated through proteins or functional DNAs (e.g., structure-switching aptamers and RNA-cleaving DNAzymes) that undergo a conformation change or cleavage reaction to release a DNA activator for CRISPR systems upon target binding. However, fine-tuning these DNA activators represents a major challenge as many activator sequences must be engineered and tested before a suitable CRISPR-based sensor can be established. Thus, strategies that can immediately transform the non-nucleic acid target recognition event into an effective output signal without the need for further optimization are highly desirable for future applications of CRISPR-Cas sensors.

So far, all reported CRISPR-based biosensing systems recruit linear CRISPR RNAs (^{L}crRNAs), which guide Cas proteins to recognize specific nucleic acid sequences; thus, triggering Cas-enzyme-mediated collateral cleavage of single-stranded (ss) DNA (ssDNA) or ssRNA reporter molecules.[3,4] In nature, covalently closed circular RNAs (circRNAs or ^{C}RNAs) have been widely reported, and are found in viroids, virusoids, spliced introns, and exons of eukaryotes, bacteria, and archaea.[5] Furthermore, post-synthetic circRNAs can be prepared by chemical or enzymatic ligation, which represents a highly unique class of NA nanostructures for various functional devices.[6] However, these naturally occurring and artificial ^{C}RNAs are rarely explored for the development of CRISPR biosensing systems, simply because they exhibit different structures and functions compared to their linear

Y. Wu, Y. Chang, M. Liu
School of Environmental Science and Technology
Key Laboratory of Industrial Ecology and Environmental Engineering (Ministry of Education)
Dalian University of Technology
Dalian POCT Laboratory
Dalian 116024, China
E-mail: mliu@dlut.edu.cn
D. Chang, Y. Li
Department of Biochemistry and Biomedical Sciences
McMaster University
1280 Main Street West, Hamilton, Ontario L8S4K1, Canada
Q. Zhang
School of Bioengineering
Dalian University of Technology
Dalian 116024, China
Y. Liu
Department of Neurology
Dalian Municipal Central Hospital
Affiliated Hospital of Dalian Medical University
Dalian 116033, China
J. D. Brennan
Biointerfaces Institute
McMaster University
1280 Main Street West, Hamilton, Ontario L8S4O3, Canada
The ORCID identification number(s) for the author(s) of this article can be found under https://doi.org/10.1002/smll.202303007

DOI: 10.1002/smll.202303007

 © 2023 Wiley-VCH GmbH

forms.[6] Therefore, we hypothesized that the formation of circular tertiary structures to create circular crRNAs (^{C}crRNAs) might serve to mask the normal function of the linear crRNAs, making them unavailable for regulating the Cas effectors.

Inspired by some natural ^{C}RNAs that undergo autocatalytic cleavage due to the existence of self-cleaving ribozymes,[7] it is expected that ^{C}crRNAs can be converted to ^{L}crRNAs using nucleic acid enzymes (NAzymes) with RNA-cleaving activities; thus, activating the CRISPR-Cas functions. To date, both nature and researchers have evolved and engineered a wide variety of RNA-cleaving NAzymes (e.g., ribozymes, DNAzymes, and aptazymes) that bind many different ligands of interest (e.g., metal ions, small molecules, oligonucleotides, proteins, and pathogenic bacteria).[8] Thus, we hypothesized that NAzymes could be used as molecular recognition elements to control the availability of ^{L}crRNA; and thus, modulate downstream CRISPR-Cas systems, resulting in a highly versatile and broadly applicable biosensing strategy for non-nucleic acid targets.

As we will show for the first time in this work, ^{C}crRNA effectively deactivates CRISPR-Cas12a activity (**Figure 1**a). Upon cleaving by RNA-cleaving NAzymes; however, the restored ^{L}crRNA can activate the CRISPR system for both site-specific dsDNA (cis) cleavage and nonspecific (trans) cleavage of fluorophore/ quencher (FQ)-labeled ssDNA reporters (FQ-ssDNA).

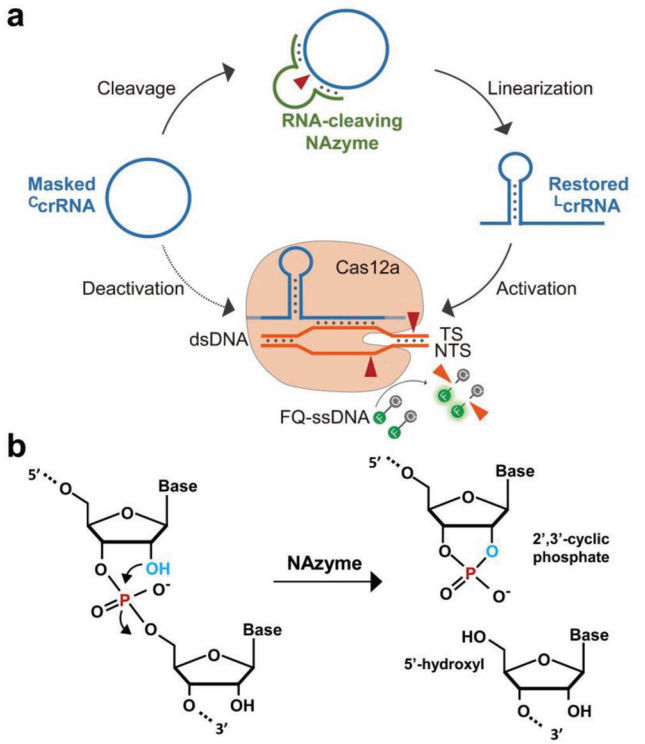


Figure 1. a) Schematic illustration of NAzyme-activated CRISPR-Cas12a with circular CRISPR RNA (NA3C). Topologically masked ^{C}crRNA was used to abrogate CRISPR-Cas12a functions, whereas RNA cleavage reactions generated ^{L}crRNA to activate the CRISPR functions. NAzyme, nucleic acid enzyme; ^{C}crRNA, circular CRISPR RNA; ^{L}crRNA, linear CRISPR RNA; dsDNA, double-stranded DNA; ssDNA, single-stranded DNA; target strand (TS); nontarget strand (NTS). b) Transesterification reaction catalyzed by NAzymes.

The NAzymes featured here catalyze the transesterification reaction between an RNA 2'-hydroxyl group and the adjacent phosphodiester linkage, resulting in the formation of 2',3'-cyclic phosphate and 5'-hydroxyl RNA termini (Figure 1b). We termed this approach NAzyme-Activated CRISPR-Cas12a with Circular CRISPR RNA (NA3C). We further demonstrate the versatility of NA3C through the design of biosensing systems for real-time and sensitive detection of a small molecule, adenosine 5'-triphosphate (ATP), and two bacterial pathogens, *Escherichia coli (E. coli)* and *Klebsiella pneumoniae* (*K. pneumoniae*). In addition, we demonstrate the applicability of NA3C with the EC1 DNAzyme for *E. coli* to test for urinary tract infections using minimally processed patient urine samples, showing high clinical sensitivity and specificity when compared to conventional plate-based assay methods.

2. Results and Discussion

2.1. Effects of ^{C}crRNAs on CRISPR-Cas12 Functions

The conceptual cornerstone of this work is the assumption that circularization efficiently blocks the function of crRNAs and CRISPR systems. To test this hypothesis, we first synthesized a 41-nucleotide (nt) ^{C}crRNA through template-directed enzymatic ligation (Figure S1, Supporting Information). We then performed Cas12a-catalyzed cis-dsDNA cleavage with gel-purified ^{C}crRNA (Figure S2, Supporting Information). dsDNA was prepared by annealing nontarget strand (NTS) to fluorophore-labeled target strand (TS). As shown in **Figure 2**a, the kinetic analysis of the cleavage reaction of Cas12a-^{C}crRNA with dsDNA gave a final yield of 16% ± 5% in 60 min. To rule out the possibility that the residual ^{L}crRNA in gel-purified ^{C}crRNA might have contributed to this weak cis-dsDNA cleavage, we used RNase R-treated ^{C}crRNA, in which the potential ^{L}crRNA was expected to be completely removed (RNase R is a 3´-to-5´ exoribonuclease that digests all linear RNAs). The nearly identical cleavage yield (18% ± 6% in 60 min, Figure S3, Supporting Information) was obtained with RNase R-treated ^{C}crRNA, suggesting that the observed weak cis-dsDNA cleavage activity was solely linked to the use of ^{C}crRNA. For comparison, we found that Cas12a-^{L}crRNA catalyzed *cis*-dsDNA cleavage at a yield of 85% ± 6% in 60 min. We next tested whether ^{C}crRNA could inhibit *trans*-ssDNA cleavage by Cas12a using FQ-ssDNA (5-nt). No significant fluorescence increase was observed for Cas12a-^{C}crRNA even in the presence of a dsDNA activator (Figure 2b). In sharp contrast, Cas12a-^{L}crRNA bound to a dsDNA activator efficiently catalyzed *trans*-ssDNA cleavage, resulting in a dramatic time-dependent increase in fluorescence. Collectively, these data indicated that ^{C}crRNAs robustly inhibited both *cis*- and *trans*-acting DNase activities of Cas12a, up to 5-fold and 30-fold, respectively. Note that this difference is presumably a result of the important feature of Cas12a: its *cis* cleavage is a process of single turnover, whereas the trans cleavage is capable of producing multiple turnovers.[3d] We further examined whether the observed blockage required a specific size of ^{C}crRNA. Expanding the size of ^{C}crRNA with 10 and 20-nt poly(adenine) or poly(uracil) spacers resulted in increased *cis*- and *trans*-cleavage activity (Figures S4 and S5, Supporting Information), suggesting that these extended ^{C}crRNAs now have acquired better topological flexibility to bind to and activate Cas12a.

© 2023 Wiley-VCH GmbH

16136829, 0, Downloaded from https://onlinelibrary.wiley.com/doi/10.1002/smll.202303007 by Hefei University Of Technology, Wiley Online Library on [10/06/2023]. See the Terms and Conditions (https://onlinelibrary.wiley.com/terms-and-conditions) on Wiley Online Library for rules of use; OA articles are governed by the applicable Creative Commons License

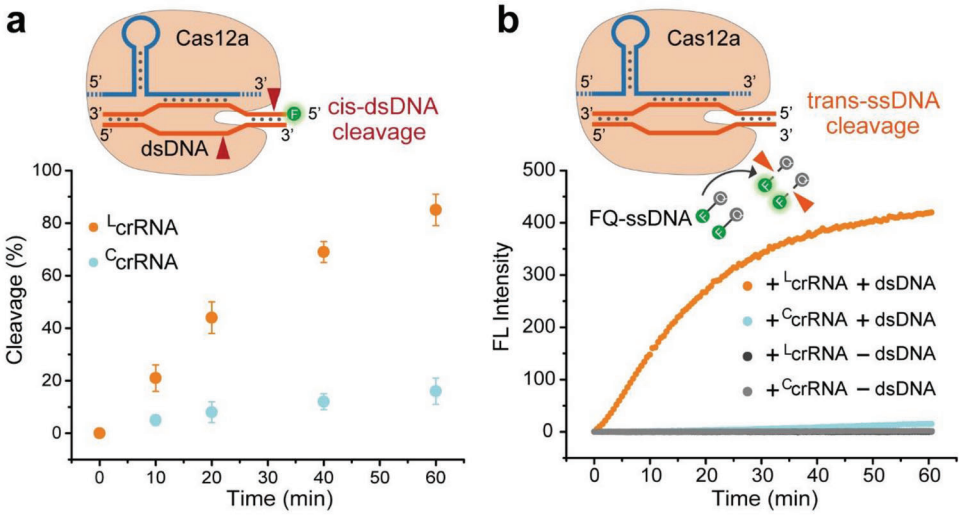


Figure 2. Effects of ^{C}crRNAs on CRISPR-Cas12a functions. Kinetics of Cas12a-^{L}crRNA (or ^{C}crRNA)-catalyzed a) cis-dsDNA cleavage and b) trans-ssDNA cleavage. Fluorophore-labeled TS (at 5' end) was used for testing site-specific dsDNA cutting. The error bars represent standard deviations of three independent experiments.

This experiment indicates that the adequate size of ^{C}crRNAs is an important factor to consider when designing a ^{C}crRNA. We also evaluated the effect of ^{C}crRNAs on Cas12a functions in the presence of ssDNA activator (Figure S6, Supporting Information). In contrast, ssDNA activators can also efficiently activate the *trans*-ssDNA cleavage activity of Cas12a-^{C}crRNA.

2.2. Interactions of crRNAs With Cas12a

Next, we studied the effects of circularization on interactions between crRNAs and Cas12a using a dot blotting assay (**Figure 3**a). Notably, ^{L}crRNA produced detectable binding to catalytically active Cas12a on nitrocellulose membranes, whereas circularization significantly reduced the binding of ^{C}crRNA to Cas12a. We then measured the apparent dissociation constants (K_d) of Cas12a for ^{L}crRNA and ^{C}crRNA using fluorescence anisotropy-based binding titrations (Figure 3b). ^{L}crRNA showed excellent binding affinity to Cas12a with a K_d of 42 ± 8 nM, while ^{C}crRNA exhibited much reduced affinity, with a K_d of 260 ± 20 nM, representing ≈sixfold affinity reduction. This result suggested that the blockage of CRISPR-Cas functions was a consequence of the disruption of interactions between ^{C}crRNAs and the Cas12a protein.

2.3. NA3C Reaction

We investigated whether RNA cleavage can trigger the linearization of ^{C}crRNAs; and thus, activate the CRISPR system. Specifically, we evaluated the use of RNA-cleaving ribozymes (RCR) and RNA-cleaving DNAzymes (RCD) in converting ^{C}crRNAs into ^{L}crRNAs. In the first experiment, we employed HH15, a small hammerhead ribozyme that is able to cleave RNA in

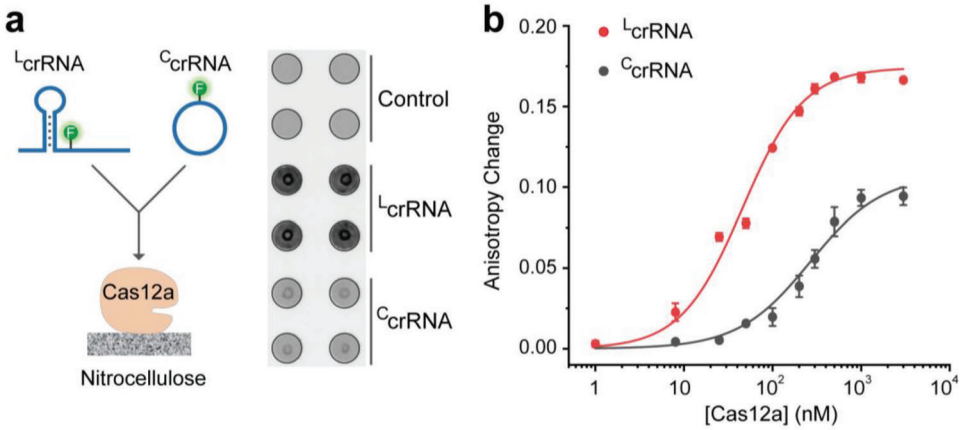


Figure 3. Interactions of crRNAs with Cas12a. a) Schematic of the dot blotting assay, and the results obtained with binding of Cas12a by the fluorophore-labeled ^{L}crRNA or ^{C}crRNA. For the control samples, no Cas12a was immobilized onto nitrocellulose membranes. b) Determination of K_d for ^{L}crRNA and ^{C}crRNA against Cas12a using the fluorescence anisotropy binding assay. The error bars represent standard deviations of three independent experiments.

© 2023 Wiley-VCH GmbH

16136829, 0, Downloaded from https://onlinelibrary.wiley.com/doi/10.1002/smll.202303007 by Hefei University Of Technology, Wiley Online Library on [10/06/2023]. See the Terms and Conditions (https://onlinelibrary.wiley.com/terms-and-conditions) on Wiley Online Library for rules of use; OA articles are governed by the applicable Creative Commons License

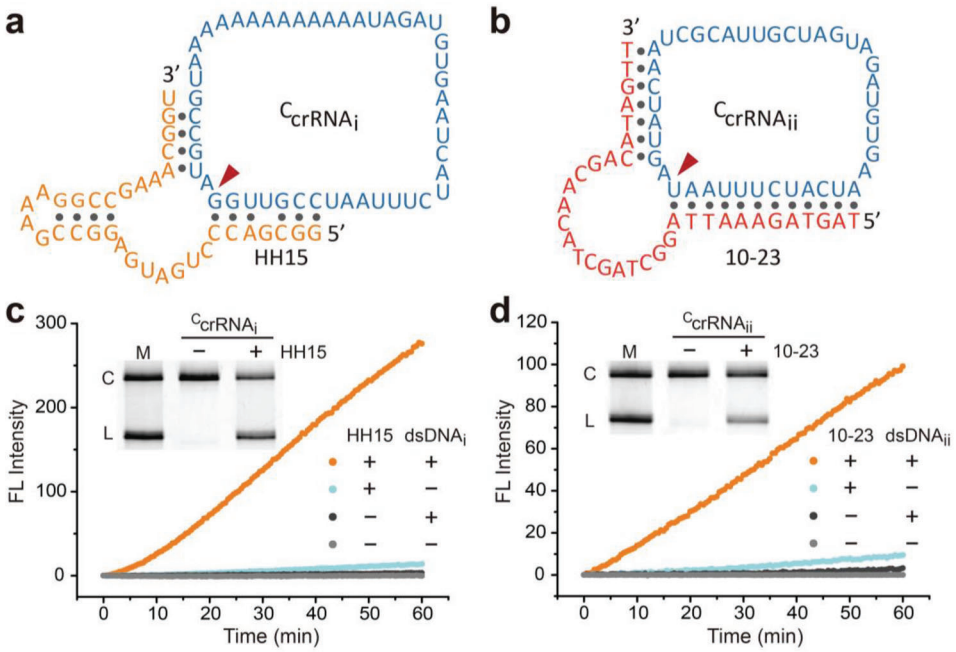


Figure 4. NA3C reaction. Sequences of a) ^{C}crRNA$_i$/HH15 and b) ^{C}crRNA$_{ii}$/10-23. Time-course analysis of FQ-ssDNA cleavage by c) Cas12a-^{C}crRNA$_i$ and d) Cas12a-^{C}crRNA$_{ii}$ in the presence of indicated components. The inset shows the cleavage of fluorophore-labeled ^{C}crRNA$_x$ (x = i or ii). The arrowhead in panels (a,b) indicates the cleavage site of ^{C}crRNA$_x$. Lane M, markers made of ^{C}crRNA$_x$ (denoted C) and ^{L}crRNA$_x$ (denoted L), x = i or ii.

trans format.[9] HH15 interacts with ^{C}crRNA$_i$ (48-nt) using two Watson–Crick binding arms and cleaves an A–G junction (**Figure 4**a). In the second experiment, we chose 10–23 deoxyribozyme, a well-known RCD capable of carrying out sequence-specific cleavage of all-RNA or chimeric RNA/DNA substrates.[10] The trans-acting 10–23 also interacted with ^{C}crRNA$_{ii}$ (41-nt) through two binding arms located on the two sides of the cleavage site (Figure 4b). Note that the cleavage reaction was conducted under single-turnover conditions with a 50-fold excess of the NAzymes over the circular crRNAs. The inset in Figure 4c (or Figure 4d) indicates that HH15 (or 10–23) indeed facilitated the cleavage of ^{C}crRNA$_i$ (or ^{C}crRNA$_{ii}$), as evidenced by the accumulation of ^{L}crRNA$_i$ (or ^{L}crRNA$_{ii}$). Note that ^{C}crRNA$_i$ (or ^{C}crRNA$_{ii}$) migrates more slowly than free ^{L}crRNA$_i$ (or ^{L}crRNA$_{ii}$). An inactive HH15 mutant, HH15M (or 10–23 mutant, 10–23 M), was also tested as a control (Figure S7, Supporting Information). No cleavage product was observed, indicating that the cleavage of each ^{C}crRNA was dependent on the functionality of the NAzyme.

Having demonstrated that each NAzyme can linearize a matching ^{C}crRNA into its ^{L}crRNA, we examined the use of the cleavage reaction mixture for activating Cas12a toward cleaving dsDNA substrates. As expected, HH15 (or 10–23)-induced cleavage of fluorophore-labeled ^{C}crRNA$_i$ (or ^{C}crRNA$_{ii}$) led to the restoration of CRISPR-Cas12a for both *cis*-dsDNA cutting (Figure S8, Supporting Information) and *trans*-ssDNA cleavage (Figure 4c,d).

2.4. NA3C for ATP and *E. Coli* Detection

We next examined the possibility of exploiting NA3C for biosensing applications. Many allosteric NAzymes or aptazymes have been reported, where catalytical activities are regulated by effectors ranging from small molecules to oligonucleotides to proteins.[8] In theory, the NA3C reaction should be compatible with any RNA-cleaving NAzymes, making it a versatile biosensing platform for detection of wide-ranging targets of interest. We designed three NA3C systems, one for detecting ATP, and the other two for sensing *E. coli* and *K. pneumoniae*, respectively. As shown in **Figure 5**a, the ATP-dependent ribozyme, named Class I(a),[11] consists of an anti-ATP RNA aptamer domain (red),[12] a hammerhead ribozyme (yellow), and a communication module (black); the sequence of ^{C}crRNA$_a$ (49-nt) was specifically designed to permit its cleavage by Class I(a) in the presence of ATP. It is noteworthy that the number of base-pairs in ^{C}crRNA$_a$/Class I(a) was optimized to produce a maximal cleavage yield (Figure S9, Supporting Information). The *E. coli*-dependent DNAzyme, EC1 (Figure 5b), was a previously isolated RCD that could only be activated by *E. coli*;[13] ^{C}crRNA$_b$ (69-nt) was designed to have a crRNA of Cas12a and an RNA-containing DNA sequence (RDS, marked in yellow) that acted as the substrate of EC1. The *K. pneumoniae*-dependent DNAzyme, KP6, could be specifically activated by *K. pneumoniae*;[14] ^{C}crRNA$_c$ (71-nt) was made of a crRNA and an RDS for KP6. Note that ^{C}crRNA$_b$ and ^{C}crRNA$_c$ contained 69 and 71 nucleotides, respectively, but could still effectively inhibit Cas12a functions (Figures S10 and S11, Supporting Information). These observations, together with the observations made with ^{C}crRNA containing 10-nt and 20-nt poly(adenine) or poly(uracil) spacers, suggest that the size and sequence context of crRNAs could play important roles in delivering inhibitory effect on CRISPR-Cas12a.

Class I(a), EC1, and KP6 were found to be able to cleave fluorophore-labeled ^{C}crRNA$_a$ (inset in Figure 5c), ^{C}crRNA$_b$ (inset in Figure 5d), and ^{C}crRNA$_c$ (insert in Figure S11, Supporting

© 2023 Wiley-VCH GmbH

16136829, 0, Downloaded from https://onlinelibrary.wiley.com/doi/10.1002/smll.202303007 by Hefei University Of Technology, Wiley Online Library on [10/06/2023]. See the Terms and Conditions (https://onlinelibrary.wiley.com/terms-and-conditions) on Wiley Online Library for rules of use; OA articles are governed by the applicable Creative Commons License

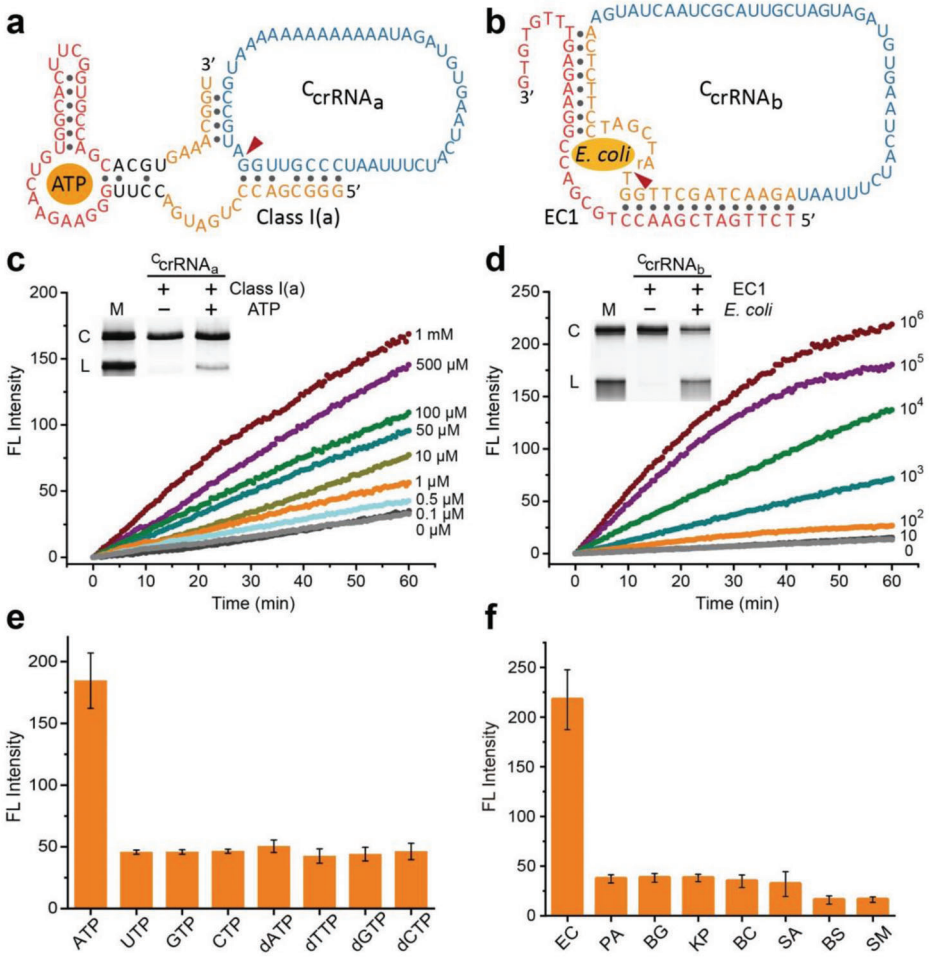


Figure 5. NA3C for ATP and *E. coli* detection. Sequences of a) ^{C}crRNA$_a$/Class I (a) and b) ^{C}crRNA$_b$/EC1 systems. Each arrowhead indicates the cleavage site. Kinetics for c) ATP detection and d) *E. coli* detection. The inset shows the cleavage of fluorophore-labeled ^{C}crRNA$_y$ (y = a or b). Lane M, markers made of ^{C}crRNA$_y$ (denoted C) and ^{L}crRNA$_y$ (denoted L), y = a or b. Specificity of e) the ATP sensor and f) the *E. coli* sensor. The error bars represent standard deviations of three independent experiments.

Information) in the presence of cognate targets. We then investigated the feasibility of performing quantitative analysis with NA3C. The NA3C reactions were monitored in real-time with FQ-ssDNA that was cleaved by Cas12a to generate fluorescence, and the maximum signal-to-noise reached nearly 5, 16, and 9-fold for ATP, *E. coli*, and *K. pneumoniae* detection, respectively. The limit of detection (LOD, defined as 3σ, σ = standard deviation of the blank samples) for the ATP, *E. coli*, and *K. pneumoniae* sensors was demonstrated to be 500 nM (Figure 5c), 10^2 CFU mL^{-1} (Figure 5d), and 10^2 CFU mL^{-1} (Figure S11, Supporting Information), respectively. Therefore, our NA3C strategy offers much better sensitivity compared with current CRISPR-based method[15] for non-nucleic acid targets (Table S2, Supporting Information). It is worth noting the LOD of the NA3C system is two orders of magnitude lower than that of NAzyme assay without signal amplification.[13b,16] Furthermore, the NA3C sensor offers a detection sensitivity that is ten times better than the commercial enzyme-linked immunosorbent assay (ELISA).[13c] We also used the Class I(a)-NA3C system to detect ATP in 10% human plasma. This is because it may contain many interfering molecules, which will increase the background signal; thus, resulting in an increased LOD of 5 μM (Figure S12, Supporting Information). We also tested against various known concentrations of *E. coli* (or *K. pneumoniae*) spiked in clinical urine samples. This assay could detect *E. coli* (or *K. pneumoniae*) at a concentration as low as 10^2 cells mL^{-1} in urine (Figure S13, Supporting Information).

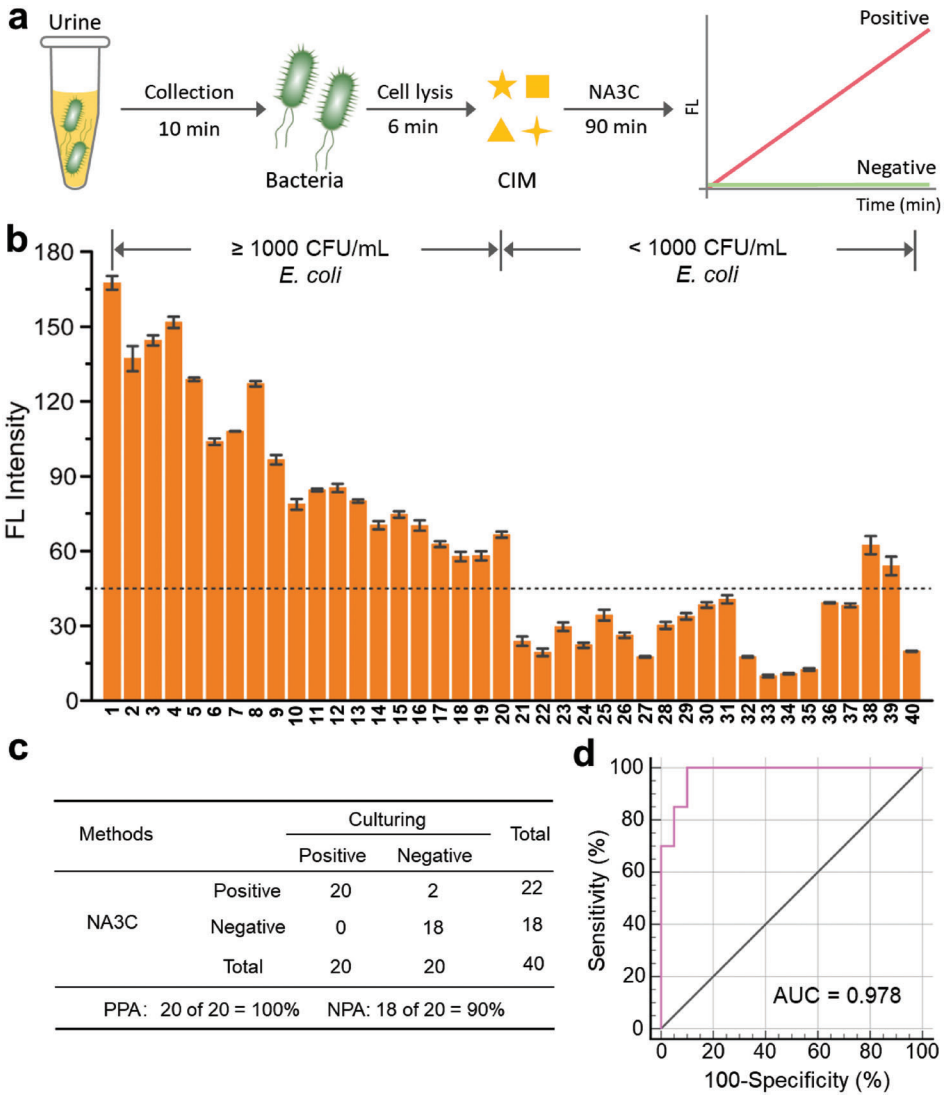
Besides the high sensitivity, each sensor also exhibited excellent selectivity. No increase of fluorescence was observed when each system was tested with unintended targets: UTP, GTP, CTP, dATP, dTTP, dGTP, and dCTP for the ATP sensor (Figure 5e); *Pseudomonas aeruginosa* (PA), *Burkholderia gladioli* (BG), *K. pneumoniae* (KP), *Bacillus cereus* (BC), *Staphylococcus aureus* (SA), *Bacillus subtilis* (BS), and *Streptococcus mutans* (SM) for the *E. coli* sensor (Figure 5f); and EC, BG, PA, BC, SA, BS, and SM for the *K. pneumoniae* sensor (Figure S14, Supporting Information).

2.5. NA3C for *E. Coli* Detection in Clinical Urine Samples

To investigate the applicability of the NA3C system in clinical diagnosis, we applied the *E. coli* sensor for the detection of *E. coli* in urine samples from patients diagnosed with urinary tract

© 2023 Wiley-VCH GmbH

16136829, 0, Downloaded from https://onlinelibrary.wiley.com/doi/10.1002/smll.202303007 by Hefei University Of Technology, Wiley Online Library on [10/06/2023]. See the Terms and Conditions (https://onlinelibrary.wiley.com/terms-and-conditions) on Wiley Online Library for rules of use; OA articles are governed by the applicable Creative Commons License



Methods		Culturing		Total
		Positive	Negative	
NA3C	Positive	20	2	22
	Negative	0	18	18
	Total	20	20	40
PPA: 20 of 20 = 100%		NPA: 18 of 20 = 90%		

Figure 6. NA3C for *E. coli* detection in clinical urine samples. a) Schematic of *E. coli* detection workflow from sample to result. CIM: crude intracellular mixture. b) Monitoring of fluorescence signal for all of the urine samples tested ($n = 40$). c) Performance characteristics of NA3C assay. A total of 40 clinical samples (20 positive and 20 negative) were evaluated using NA3C and standard culturing method. PPA, positive predictive agreement; NPA, negative predictive agreement. d) Receiver operator characteristic (ROC) curves of the assays showing the detection accuracies. The error bars represent standard deviations of three independent experiments.

infections (UTIs). The sensor was used to achieve *E. coli* detection with patient urine samples without culturing steps. The overall assay procedure, shown in **Figure 6**a, includes: 1) bacterial cells in samples were collected by centrifugation (10 min); 2) Cells were lysed (6 min); 3) the NA3C reaction was performed (90 min); and 4) the fluorescence signal was acquired (1 min). Using this procedure, we analyzed 20 *E. coli* culturing-positive and 20 *E. coli* culturing-negative samples (Figure S15, Supporting Information). Based on the commonly used clinical threshold of 1000 CFU mL^{-1},[17] the positive predictive agreement (PPA) and negative predictive agreement (NPA) of the NA3C sensor relative to the standard culturing method were 100% and 90%, respectively. An area under the curve (AUC) of 0.978 was obtained for the receiver operator characteristic (ROC) plot. These excellent values point to the utility of NA3C for clinical diagnosis.

3. Conclusion

In summary, we have demonstrated a versatile biosensing strategy that uniquely integrates CRISPR-Cas12a with RNA-cleaving NAzymes for sensitive detection of wide-ranging non-nucleic acid targets. The approach begins with a post-synthetic ^{C}crRNA that blocks the CRISPR-Cas12a functions, whereas NAzyme-mediated RNA cleavage activates the CRISPR system. To our knowledge, this work serves as the first example of topology-controlled CRISPR-Cas functions achieved through crRNA engineering. The broad utility of this approach is illustrated though engineering three sensors that are capable of achieving sensitive detection of a small-molecule analyte and two bacterial pathogens. Clinical evaluation of one sensor using 40 patient urine samples demonstrated a clinical sensitivity of 100%,

© 2023 Wiley-VCH GmbH

16136829, 0, Downloaded from https://onlinelibrary.wiley.com/doi/10.1002/smll.202303007 by Hefei University Of Technology, Wiley Online Library on [10/06/2023]. See the Terms and Conditions (https://onlinelibrary.wiley.com/terms-and-conditions) on Wiley Online Library for rules of use; OA articles are governed by the applicable Creative Commons License

specificity of 90%, and an AUC of 0.978. Given that there is a wide variety of RNA-cleaving NAzymes that bind many different molecules of interest,[1b] and that a specific ^{C}crRNA can be easily engineered through simple incorporation of RNA substrates for matching NAzymes, we envision the described strategy can significantly expand CRISPR systems for the detection of diverse targets and use them to assist clinical diagnosis of infectious and non-infectious diseases. Future work will develop a fully printed paper-based analytical device for point of care or on-site applications under resource-limited settings.[18]

4. Experimental Section

Oligonucleotides and Materials: The sequences of all DNA and RNA oligonucleotides are provided in Table S1, Supporting Information. The DNA oligonucleotides were purchased from Sangon Biotech (Shanghai, China), and purified by 10% denaturing (8 M urea) polyacrylamide gel electrophoresis (dPAGE) or high performance liquid chromatography (HPLC). The RNA oligonucleotides were purchased from General Biotech (Shanghai, China), and purified by high performance liquid chromatography (HPLC). T4 RNA ligase 2 (T4RL2) was purchased from Beyotime Biotechnology (Shanghai, China). Engen Lba Cas12a protein was purchased from New England Biolabs. Adenosine 5'-triphosphate (ATP), cytidine 5'-triphosphate (CTP), guanosine 5'-triphosphate (GTP), uridine 5'-triphosphate (UTP), Deoxyadenosine 5'-triphosphate (dATP), Deoxycytidine 5'-triphosphate (CTP), Deoxyguanosine 5'-triphosphate (GTP), Deoxythymidine 5'-triphosphate (dTTP), and RNase inhibitor were purchased from Sangon Biotech (Shanghai, China). Nuclease-free water was purchased from TaKaRa Biomedical Technology (Dalian, China). RNAse R was purchased from Lucigen Biosearch Technologies. All other chemicals were purchased from Sigma–Aldrich and used without further purification. Cystine-lactose-electrolyte-deficient (CLED) medium was purchased from Solarbio Life sciences (Beijing, China). *E. coli* (CICC 23796), *K. pneumoniae* (ATCC 13883), *P. aeruginosa* (ATCC 9027), *B. gladioli* (CICC 10574), *B. cereus* (CICC 10352), *S. aureus* (ATCC 6538), and *B. subtilis* (CICC 10002) were purchased from the China Center of Industrial Culture Collection (CICC). *S. mutans* (CGMCC 1.2499) was purchased from the China General Microbiological Culture Collection Center (CGMCC). All the human blood and urine samples were acquired from the Dalian Municipal Central Hospital.

Buffers used in this work:

1× hybridization buffer (1× HB): 20 nM Tris-HCl, pH 7.5, 100 mM KCl, 5 mM $MgCl_2$.
1× EC1 reaction buffer (1× ERB): 50 mM HEPES, pH 7.5, 150 mM NaCl, 15 mM $MgCl_2$.
1× Cas12a cleavage buffer (1× CCB): 20 mM Tris-HCl, pH 7.5, 100 mM KCl, 5 mM $MgCl_2$, 1 mM DTT, 5% glycerol, 50 μg mL^{-1} Heparin.
1× binding buffer (1× BB): 20 mM Tris-HCl, pH 7.5, 100 mM KCl, 5 mM $MgCl_2$, 1 mM DTT, 5% glycerol, 50 μg mL^{-1} heparin, 50 μg mL^{-1} BSA, 0.01% v/v IGEPAL CA-630.
1× washing buffer (1× WB): 50 mM HEPES, pH 7.5, 100 mM KCl, 5 mM $MgCl_2$, and 0.01% v/v IGEPAL CA-630.
1× RNAse R buffer (1× RRB): 20 mM Tris-HCl, pH 8.0, 100 mM KCl, 0.1 mM $MgCl_2$.
1× KP6 reaction buffer (1× KRB): 50 mM HEPES, pH 7.5, 150 mM NaCl, 15 mM $MgCl_2$, and 0.01% Tween 20.

Apparatus: The fluorescence images were obtained using a Typhoon 5 variable mode imager (GE Healthcare) and analyzed using Image Quant software (Molecular Dynamics). Fluorescence measurements were performed with a Cary Eclipse fluorescence spectrophotometer. The fluorescence polarization was monitored on a Tecan Spark microplate reader (Switzerland). The UV–vis absorbance was measured with a Cary 100 UV–vis spectrophotometer.

Preparation of Circular crRNA (^{C}crRNA): 5′-phosphorylated linear crRNA (such as ^{L}crRNA$_i$, 100 pmol) was first mixed with ligation template (such as LT$_i$, 110 pmol) and 10 μL of 10× T4RL2 buffer (500 mM Tris-HCl, 20 mM $MgCl_2$, 10 mM DTT, and 4 mM ATP) heated to 90 °C for 2 min; and then, cooled at room temperature (RT) for 15 min. To this mixture, 50 U (units) of T4RL2, 100 U (units) of RNase inhibitor, and nuclease-free water were added to a total volume of 100 μL. After incubation at 37 °C for 2 h, the obtained ^{C}crRNA molecules were concentrated by standard ethanol precipitation and purified by 10% dPAGE (8 M urea). Note that LT$_{ii}$ (18 nt) was used as the ligation template for ^{L}crRNA$_{ii}$ (51 nt) and ^{L}crRNA$_{ii}$ (61 nt).

Preparation of Double-Stranded DNA (dsDNA): In a typical experiment, dsDNA activators were prepared by annealing fivefold molar excess of the non-target strand (NTS) to target strand (TS) in 1× HB at 95 °C for 5 min, followed by gradient cooling (1 °C min^{-1}) to RT.

Preparation of Crude Intracellular Mixture (CIM): *E. coli*, *P. aeruginosa*, *B. gladioli*, *B. cereus*, *S. aureus*, and *B. subtilis* were grown overnight in 5 mL of Luria Bertani (LB); *S. mutans* was grown overnight in 5 mL of brain heart infusion broth (BHIB); *K. pneumoniae* was grown overnight in 5 mL of Tryptic Soy Broth (TSB) with continuous shaking at 37 °C until the culture reached an OD_{600} of ≈1. 1 mL of this culture was centrifuged at 11 000 × *g* for 10 min at 4 °C. The cell pellet was suspended in 100 μL of 1× ERB at 0 °C. The bacteria cells were sonicated for 1 min and then centrifuged at 11 000 × g for 10 min at 4 °C. The obtained CIM was used for the following experiment.

Kinetics of Cas12a-^{L}crRNA (or ^{C}crRNA)-Catalyzed Site-Specific dsDNA (Cis) Cleavage: FAM-labeled TS$_{ii}$ (at 5' end) and NTS$_{ii}$ were used for the preparation of dsDNA$_{ii}$. Cas12a (5 pmol) was pre-assembled with either ^{C}crRNA$_{ii}$ (41 nt) or ^{L}crRNA$_{ii}$ (2.5 pmol) at RT for 10 min in 50 μL of 1× CCB containing 1 U μL^{-1} RNase inhibitor. 1.25 μL of 2 μM FAM-labeled dsDNA activator was added to the mixture and incubated at 37 °C for 10, 20, 40, and 60 min, before heating at 90 °C for 10 min to deactivate Cas12a. The reaction mixtures were analyzed by 15% denatured polyacrylamide gel electrophoresis.

Kinetics of Cas12a-^{L}crRNA (or ^{C}crRNA)-Catalyzed Nonspecific ssDNA (Trans) Cleavage: Cas12a (10 pmol) was first mixed with dsDNA$_{ii}$ (10 pmol), ^{C}crRNA$_{ii}$, or ^{L}crRNA$_{ii}$ (2.5 pmol) at 37 °C for 30 min in 50 μL of 1× CCB containing 1 U μL^{-1} RNase inhibitor. 3.75 μL of 10 μM FQ-ssDNA reporter was added, followed by measurement of fluorescence intensity for 60 min at 37 °C using a Cary Eclipse spectrofluorimeter with fluorescence measurements taken every 30 s (λ_{ex}: 495 nm; λ_{em}: 520 nm).

Dot Blotting Assay: Wax-printed paper plates (Millipore HF120 nitrocellulose membrane) were used with the diameter of each test zone being 4 mm. Wax was printed using a Xerox ColorQube 8570 N solid wax printer followed by heating at 120 °C for 2 min to melt the wax through the membrane. A total of 1 μL of Cas12a (148 ng uL^{-1}) was first spotted onto each test zone. After drying at room temperature for 10 min, the membrane was blocked with 10 μL of 1% BSA in 1× BB for 30 min. After washing twice with 20 μL of 1× WB, 10 μL of 100 nM FAM-labeled ^{L}crRNA$_i$ or ^{C}crRNA$_i$ was added and incubated for 30 min. The paper plate was placed in a trough containing 2 mL of 1× WB for 5 min. The paper was then dried at RT and the fluorescence of each zone scanned and quantified.

Fluorescence Polarization Assay: Binding reactions were performed in 100 μL of 1× BB containing 5 nM FAM-labeled ^{L}crRNA$_i$ (or ^{C}crRNA$_i$), different concentrations of Cas12a, and 1 U μL^{-1} RNase inhibitor. After incubation at 37 °C for 30 min, the fluorescence anisotropy values were measured by a microplate reader with an excitation wavelength of 485 nm and an emission wavelength of 520 nm. K_d values were obtained by fitting the fluorescence anisotropy change to a one-site saturation ligand binding equation using the non-linear regression.

NA3C Reaction: For studying the cleavage of ^{C}crRNA$_i$ (or ^{C}crRNA$_{ii}$) by HH15 (or 10–23), FAM-labeled ^{C}crRNA$_i$ (or ^{C}crRNA$_{ii}$) was used. In a typical experiment for NA3C reactions, 1.25 μL of 2 μM ^{C}crRNA$_i$ (or ^{C}crRNA$_{ii}$) was mixed with 1.25 μL of 100 μM HH15 (or 10–23), 2 μL of 500 mM Tris-HCl (pH 7.5), and 5 μL of ddH_2O, and heated at 90 °C for 3 min before being cooled to RT. This was followed by the addition of 10 μL of 100 mM $MgCl_2$ and 0.5 μL of RNase inhibitor (40 U μL^{-1}) to a total volume of 20 μL. The reaction mixture was then incubated at RT for 60 min. 10 μL of the above cleavage mixture was mixed with 10 μL of 2× RNA loading buffer

© 2023 Wiley-VCH GmbH

16136829, 0, Downloaded from https://onlinelibrary.wiley.com/doi/10.1002/smll.202303007 by Hefei University Of Technology, Wiley Online Library on [10/06/2023]. See the Terms and Conditions (https://onlinelibrary.wiley.com/terms-and-conditions) on Wiley Online Library for rules of use; OA articles are governed by the applicable Creative Commons License

(95% v/v formamide, 0.02% w/v SDS, 0.02% w/v bromophenol blue, and 0.01% w/v xylene cyanol) containing 1 mM EDTA. The mixture was then run on a 20% dPAGE gel. The gel was scanned and analyzed by Image Quant software. 20 µL of the above cleavage mixture was mixed with 5 µL of 10× CCB, 1.25 µL of RNase inhibitor (40 U μL^{-1}), 1 µL of 10 µM Cas12a, and 1 µL of 10 µM $dsDNA_i$ (or $dsDNA_{ii}$). After incubation at 37 °C for 30 min, 18 µL of nuclease-free water and 3.75 µL of 10 µM FQ-ssDNA were added (total volume: 50 µL). Fluorescence intensity was measured for 60 min at 37 °C as described above.

NA3C Reaction for ATP Detection: For studying the cleavage of $^{C}crRNA_a$ by Class I (a), FAM-labeled $^{C}crRNA_a$ was used. In a typical experiment for ATP detection, 1.25 µL of 2 µM $^{C}crRNA_a$, 2 µL of 500 mM Tris-HCl (pH 7.5), 1.25 µL of 100 µM Class I (a), and 12 µL of ddH_2O were heated at 90 °C for 3 min. After cooling to RT, 2 µL ATP with various concentrations (0, 1, 5, 10, 100, 500, 1000, 5000, and 10 000 µM),1 µL of 100 mM $MgCl_2$, and 0.5 µL of RNase inhibitor (40 U μL^{-1}) were added and then incubated at RT for 60 min. 20 µL of the above cleavage mixture was mixed with 5 µL of 10× CCB, 1.25 µL of RNase inhibitor (40 U μL^{-1}), 1 µL of 10 µM Cas12a, and 1 µL of 10 µM $dsDNA_i$. After incubation at 37 °C for 30 min, 18 µL of nuclease-free water and 3.75 µL of 10 µM FQ-ssDNA were added (total volume: 50 µL). Fluorescence intensity was measured for 60 min at 37 °C. For studying the specificity, 1 mM UTP, GTP, CTP, dATP, dTTP, dGTP, and dCTP were used.

NA3C Reaction for E. coli Detection: For studying the cleavage of $^{C}crRNA_b$ by EC1, FAM-labeled $^{C}crRNA_b$ was used. In a typical experiment, 10 µL of 2× ERB, 1.25 µL of 2 µM $^{C}crRNA_b$, 1.25 µL of 100 µM EC1, and 1 µL of nuclease-free water were mixed and heated at 90 °C for 3 min before cooling to RT. This was followed by the addition of 1.5 µL of RNase inhibitor (40 U μL^{-1}) and 5 µL of CIM-EC at different concentration (10^7, 10^6, 10^5, 10^4, 10^3, 10^2, and 0 CFU per mL). The reaction mixture was then incubated at RT for 30 min. 20 µL of the above cleavage mixture was mixed with 5 µL of 10× CCB, 1.25 µL of RNase inhibitor (40 U μL^{-1}), 1 µL of 10 µM Cas12a, and 1 µL of 10 µM $dsDNA_{ii}$. After incubation at 37 °C for 30 min, 18 µL of nuclease-free water and 3.75 µL of 10 µM FQ-ssDNA were added (total volume: 50 µL). The reaction mixture was incubated in a fluorescence spectrophotometer for 60 min at 37 °C. For studying the specificity, CIM-PA, CIM-BG, CIM-KP, CIM-BC, CIM-SA, CIM-BS, and CIM-SM (10^6 CFU per mL) were used.

4.0.0.1. Coli Detection from Clinical Urine Samples by NA3C: 1) Cell collection: the bacterial cells in samples (1 mL) were collected by centrifugation at 11 000 × *g* for 10 min. 2) Cell lysis: after washing twice with 1× ERB, the cell pellet was suspended in 100 µL of 1× ERB at 0 °C and sonicated for 1 min. The cell suspension was then centrifuged at 11 000 × *g* for 5 min at 4 °C to obtain CIM-EC. 3) NA3C: 5 µL of CIM-EC, 10 µL of 2× ERB, 1.25 µL of 2 µM $^{C}crRNA_b$, 1.25 µL of 100 µM EC1, 1 µL of nuclease-free water, and 1.5 µL of RNase inhibitor (40 U μL^{-1}) were incubated at RT for 30 min. 20 µL of the above cleavage mixture was then mixed with 5 µL of 10× CCB, 1.25 µL of RNase inhibitor (40 U μL^{-1}), 1 µL of 10 µM Cas12a, and 1 µL of 10 µM $dsDNA_{ii}$. After incubation at 37 °C for 30 min, 18 µL of nuclease-free water and 3.75 µL of 10 µM FQ-ssDNA were added (total volume: 50 µL). The reaction mixture was incubated in a fluorescence spectrophotometer for 30 min at 37 °C.

Statistical Analysis: Origin 2018 (OriginLab, USA) was used for statistical analysis. Data were presented either as the original data or as the mean ± standard error (S.E.M), $n = 3$.

Supporting Information

Supporting Information is available from the Wiley Online Library or from the author.

Acknowledgements

This work was supported by the National Natural Science Foundation of China (NSFC; Grant No. 21922601) and the Fundamental Research Funds for the Central Universities (DUT22YG217).

Conflict of Interest

The authors declare no conflict of interest.

Data Availability Statement

The data that support the findings of this study are available from the corresponding author upon reasonable request.

Keywords

aptazymes, CRISPR-Cas12a, deoxyribozymes, pathogenic bacterias, ribozymes

Received: May 21, 2023
Revised: June 1, 2023
Published online:

[1] a) L. Li, S. Xu, H. Yan, X. Li, H. S. Yazd, X. Li, T. Huang, C. Cui, J. Jiang, W. Tan, *Angew. Chem., Int. Ed.* **2021**, *60*, 2221; b) E. M. McConnell, I. Cozma, Q. Mou, J. D. Brennan, Y. Lu, Y. Li, *Chem. Soc. Rev.* **2021**, *50*, 8954; c) E. M. McConnell, I. Cozma, D. Morrison, Y. Li, *Anal. Chem.* **2020**, *92*, 327.

[2] a) M. Jinek, K. Chylinski, I. Fonfara, M. Hauer, J. A. Doudna, E. Charpentier, *Science* **2012**, *337*, 816; b) M. Kaminski, O. Abudayyeh, J. Gootenberg, F. Zhang, J. Collins, *Nat. Biomed. Eng.* **2021**, *5*, 643; c) Y. Dai, Y. Wu, G. Liu, J. J. Gooding, *Angew. Chem., Int. Ed.* **2020**, *59*, 20754; d) Z. Weng, Z. You, J. Yang, N. Mohammad, M. Lin, Q. Wei, X. Gao, Y. Zhang, *Angew. Chem., Int. Ed.* **2023**, *62*, e202214987; e) M. Broto, M. M. Kaminski, C. Adrianus, N. Kim, R. Greensmith, S. Dissanayake-Perera, A. J. Schubert, X. Tan, H. Kim, A. S. Dighe, J. J. Collins, M. M. Stevens, *Nat. Nanotechnol.* **2022**, *17*, 1120; f) P. Fozouni, S. Son, M. Díaz de León Derby, G. J. Knott, C. N. Gray, M. V. D'Ambrosio, C. Zhao, N. A. Switz, G. R. Kumar, S. I. Stephens, D. Boehm, C. L. Tsou, J. Shu, A. Bhuiya, M. Armstrong, A. R. Harris, P. Y. Chen, J. M. Osterloh, A. Meyer-Franke, B. Joehnk, Walcott K., A. Sil, C. Langelier, K. S. Pollard, E. D. Crawford, A. S. Puschnik, M. Phelps, A. Kistler, J. L. DeRisi, J. A. Doudna, et al., *Cell* **2021**, *184*, 323; g) J. Arizti-Sanz, A. Bradley, Y. B. Zhang, C. K. Boehm, C. A. Freije, M. E. Grunberg, T. F. Kosoko-Thoroddsen, N. L. Welch, P. P. Pillai, S. Mantena, G. Kim, J. N. Uwanibe, O. G. John, P. E. Eromon, G. Kocher, R. Gross, J. S. Lee, L. E. Hensley, B. L. MacInnis, J. Johnson, M. Springer, C. T. Happi, P. C. Sabeti, C. Myhrvold, *Nat. Biomed. Eng.* **2022**, *6*, 932.

[3] a) K. Pardee, A. A. Green, M. K. Takahashi, D. Braff, G. Lambert, J. W. Lee, T. Ferrante, D. Ma, N. Donghia, M. Fan, N. M. Daringer, I. Bosch, D. M. Dudley, D. H. O'Connor, L. Gehrke, J. J. Collins, *Cell* **2016**, *165*, 1255; b) J. S. Gootenberg, O. O. Abudayyeh, J. W. Lee, P. Essletzbichler, A. J. Dy, J. Joung, V. Verdine, N. Donghia, N. M. Daringer, C. A. Freije, C. Myhrvold, R. P. Bhattacharyya, J. Livny, A. Regev, E. V. Koonin, D. T. Hung, P. C. Sabeti, J. J. Collins, F. Zhang, *Science* **2017**, *356*, 438; c) J. S. Gootenberg, O. O. Abudayyeh, M. J. Kellner, J. Joung, J. J. Collins, F. Zhang, *Science* **2018**, *360*, 439; d) J. S. Chen, E. Ma, L. B. Harrington, M. Da Costa, X. Tian, J. M. Palefsky, J. A. Doudna, *Science* **2018**, *360*, 436; e) A. Ghouneimy, M. Mahfouz, *Nat. Biomed. Eng.* **2022**, *6*, 925; f) N. Mohammad, S. S. Katkam, Q. Wei, *Angew. Chem., Int. Ed.* **2022**, *61*, e202213920; g) J. Liu, H. Wang, L. Zhang, Y. Lu, X. Wang, M. Shen, N. Li, L. Feng, J. Jing, B. Cao, X. Zou, J. Cheng, Y. Xu, *Small* **2022**, *18*, 2200854.

[4] a) M. Liang, Z. Li, W. Wang, J. Liu, L. Liu, G. Zhu, L. Karthik, M. Wang, K. F. Wang, Z. Wang, J. Yu, Y. Shuai, J. Yu, L. Zhang, Z. Yang, C. Li, Q.

© 2023 Wiley-VCH GmbH

16136829, 0, Downloaded from https://onlinelibrary.wiley.com/doi/10.1002/smll.202303007 by Hefei University Of Technology, Wiley Online Library on [10/06/2023]. See the Terms and Conditions (https://onlinelibrary.wiley.com/terms-and-conditions) on Wiley Online Library for rules of use; OA articles are governed by the applicable Creative Commons License

Zhang, T. Shi, L. Zhou, F. Xie, H. Dai, X. Liu, J. Zhang, G. Liu, Y. Zhuo, B. Zhang, C. Liu, S. Li, X. Xia, Y. Tong, et al., *Nat. Commun.* **2019**, *10*, 3672; b) R. S. Iwasaki, R. T. Batey, *Nucleic Acids Res.* **2020**, *48*, e101; c) Y. Dai, R. A. Somoza, L. Wang, J. F. Welter, Y. Li, A. I. Caplan, C. C. Liu, *Angew. Chem., Int. Ed.* **2019**, *58*, 17399; d) Y. Xiong, J. Zhang, Z. Yang, Q. Mou, Y. Ma, Y. Xiong, Y. Lu, *J. Am. Chem. Soc.* **2020**, *142*, 207; e) J. Shen, X. Zhou, Y. Shan, H. Yue, R. Huang, J. Hu, D. Xing, *Nat. Commun.* **2020**, *11*, 267; f) W. Feng, A. M. Newbigging, J. Tao, Y. Cao, H. Peng, C. Le, J. Wu, B. Pang, J. Li, D. L. Tyrrell, H. Zhang, X. C. Le, *Chem. Sci.* **2020**, *12*, 4683. g) Y. Ma, Q. Mou, P. Yan, Z. Yang, Y. Xiong, D. Yan, C. Zhang, X. Zhu, Y. Lu, *Chem. Sci.* **2021**, *12*, 11740; h) S. Chen, R. Wang, S. Peng, S. Xie, C. Lei, Y. Huang, Z. Nie, *Chem. Sci.* **2022**, *13*, 2011; i) Y. Lv, Y. Sun, Y. Zhou, I. M. Khan, S. Niazi, L. Yue, Y. Zhang, Z. Wang, *Small* **2023**, *19*, 2206105; j) R. Fu, Y. Xianyu, *Small* **2023**, *19*, 2300057.

[5] a) L. Koch, *Nat. Rev. Genet.* **2017**, *18*, 272; b) L. L. Chen, *Nat. Rev. Mol. Cell Biol.* **2020**, *21*, 475; c) L. S. Kristensen, M. S. Andersen, L. V. W. Stagsted, K. K. Ebbesen, T. B. Hansen, J. Kjems, *Nat. Rev. Genet.* **2019**, *20*, 675; d) W. R. Jeck, N. E. Sharpless, *Nat. Biotechnol.* **2014**, *32*, 453.

[6] a) J. Li, M. Mohammed-Elsabagh, F. Paczkowski, Y. Li, *ChemBioChem* **2020**, *21*, 1547; b) E. Lasda, R. Parker, *RNA* **2014**, *20*, 1829; c) M. G. Mohsen, E. T. Kool, *Acc. Chem. Res.* **2016**, *49*, 2540.

[7] a) T. R. Cech, B. L. Bass, *Annu. Rev. Biochem.* **1986**, *55*, 599; b) A. C. Forster, R. H. Symons, *Cell* **1987**, *49*, 211.

[8] a) M. Famulok, J. S. Hartig, G. Mayer, *Chem. Rev.* **2007**, *107*, 3715; b) J. Liu, Z. Cao, Y. Lu, *Chem. Rev.* **2009**, *109*, 1948; c) D. Chang, S. Zakaria, S. E. Samani, Y. Chang, C. D. M. Filipe, L. Soleymani, J. D. Brennan, M. Liu, Y. Li, *Acc. Chem. Res.* **2021**, *54*, 3540; d) M. Liu, D. Chang, Y. Li, *Acc. Chem. Res.* **2017**, *50*, 2273; e) W. Zhou, R. Saran, J. Liu, *Chem. Rev.* **2017**, *117*, 8272; f) M. C. Maurel, F. Leclerc, G. Hervé, *Chem. Rev.* **2020**, *120*, 4898.

[9] M. J. Fedor, O. C. Uhlenbeck, *Biochemistry* **1992**, *31*, 12042.

[10] S. W. Santoro, G. F. Joyce, *Biochemistry* **1998**, *37*, 13330.

[11] G. A. Soukup, R. R. Breaker, *RNA* **1999**, *5*, 1308.

[12] M. Sassanfar, J. W. Szostak, *Nature* **1993**, *364*, 550.

[13] a) M. M. Ali, S. D. Aguirre, H. Lazim, Y. Li, *Angew. Chem., Int. Ed.* **2011**, *50*, 3751; b) S. D. Aguirre, M. M. Ali, B. J. Salena, Y. Li, *Biomolecules* **2013**, *3*, 563; c) M. Liu, Q. Zhang, Z. Li, J. Gu, J. D. Brennan, Y. Li, *Nat. Commun.* **2016**, *7*, 12074.

[14] M. M. Ali, A. Slepenkin, E. Peterson, W. Zhao, *ChemBioChem* **2019**, *20*, 906.

[15] a) Q. Bao, J. Sun, X. Fu, L. Sheng, Y. Ye, J. Ji, Y. Zhang, J. Wang, J. Ping, X. Sun, *Small* **2023**, 2207343; b) X. Zhang, Y. Shi, G. Chen, D. Wu, Y. Wu, G. Li, *Small Methods* **2022**, *6*, 2200794; c) H. Yang, R. Ledesma-Amaro, H. Gao, Y. Ren, R. Deng, *Biosens. Bioelectron.* **2023**, *228*, 115189; d) X. Cheng, Y. Li, J. Kou, D. Liao, W. Zhang, L. Yin, S. Man, L. Ma, *Biosens. Bioelectron.* **2022**, *215*, 114559.

[16] M. Levy, A. D. Ellington, *Chem. Biol.* **2002**, *9*, 417.

[17] A. L. Flores-Mireles, J. N. Walker, M. Caparon, S. J. Hultgren, *Nat. Rev. Microbiol.* **2015**, *13*, 269.

[18] a) Y. Zhang, Q. Zhang, F. Cheng, Y. Chang, M. Liu, Y. Li, *Chem. Sci.* **2021**, *12*, 8282; b) M. Liu, C. Y. Hui, Q. Zhang, J. Gu, B. Kannan, S. Jahanshahi-Anbuhi, C. D. M. Filipe, J. D. Brennan, Y. Li, *Angew. Chem., Int. Ed.* **2016**, *55*, 2709; c) M. Liu, Q. Zhang, B. Kannan, G. A. Botton, J. Yang, L. Soleymani, J. D. Brennan, Y. Li, *Angew. Chem., Int. Ed.* **2018**, *57*, 12440.

© 2023 Wiley-VCH GmbH

16136829, 0, Downloaded from https://onlinelibrary.wiley.com/doi/10.1002/smll.202303007 by Hefei University Of Technology, Wiley Online Library on [10/06/2023]. See the Terms and Conditions (https://onlinelibrary.wiley.com/terms-and-conditions) on Wiley Online Library for rules of use; OA articles are governed by the applicable Creative Commons License